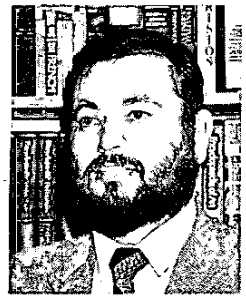

Naftali (Tuli) Herscovici
AnTeg
52 Agnes Drive
Framingham, MA 01901 USA
+1 (508) 788-5152
+1 (508) 788-6226 (Fax)
tuli@ieee.org (e-mail)

Christos Christodoulou
Department of Electrical and
Computer Engineering
University of New Mexico
Albuquerque, NM 87131-1356 USA
+1 (505) 277-6580
+1 (505) 277-1439 (Fax)
christos@eece.unm.edu (e-mail)

On The Design of Switched-Beam Wideband Base Stations

Eleftheria Siachalou[1], Elias Vafiadis[2], Sotirios S. Goudos[2], Theodoros Samaras[2], Christos S. Koukourlis[3], and Stavros Panas[1]

[1]Telecommunications Laboratory, Department of Electrical and Computer Engineering, Aristotle University of Thessaloniki
54124 Thessaloniki, Greece

[2]Radiocommunications Laboratory, Department of Physics, Aristotle University of Thessaloniki
54124 Thessaloniki, Greece

[3]Telecommunications Laboratory, Department of Electrical and Computer Engineering, Democritus University of Thrace
67100 Xanthi, Greece

Abstract

A switched-beam base-station antenna is presented. The antenna is an improvement on the Butler matrix. The input ports of the antenna are excited with equal or unequal amplitudes. The feed network is analyzed and presented in a simple manner. The antenna comprises the main part of a base station, and is useful for broadband communications. The architecture of the base station is described, and the services that can be provided are given. Finally, comments are made about the tradeoffs and benefits of the antenna in comparison to the classical Butler-matrix switched-beam and adaptive arrays.

Keywords: Smart antennas; signal processing antennas; adaptive arrays; Butler matrix; land mobile radio equipment; land mobile radio cellular systems; broadband communication; wireless networks

1. Introduction

The requirements of the appropriate quality of service and the exponentially escalating number of users force the wireless-communications industry to improve the reliability and capacity of their systems. A classical method for increasing capacity is to add macro- or micro-base stations, and to extend bandwidth. It is well known that new sites create new operational expenses, with increased management complexity. One could instead redesign the base stations and make them capable of meeting the above requirements. The use of "smart antennas" can improve wireless performance.

Smart antennas may contain switched-beam or fully adaptive configurations that electronically steer the pattern toward an individual user. Obviously, the system distinguishes the users that stand at different angular positions and, as a result, expands its capacity. The space-division multiple access (SDMA) technique starts to become highly attractive for wireless systems. A feed network that provides the proper excitation to elements of an antenna array can steer the beam to the desired direction. The so-called "beamforming network" (BFN) is implemented at the RF or at the IF stage of the transceiver unit. A switched-beam array creates fixed, multiple, and simultaneous beams. An adaptive-beam array makes use of beamforming networks that dynamically

change the array pattern. This pattern can simultaneously reject the interfering signals and receive the desired signals. In the above arrays, a multi-polarized capability can also be applied to greatly improve the capacity of the system. Adaptive arrays alter the pattern by utilizing sophisticated signal-processing algorithms. In the literature, one can find several textbooks, special issues, and research papers in the area of smart antennas [1-7].

2. Wideband Asymmetric Wireless Networks

Nowadays, there is an increasing demand for broadband services. Broadcasting or multicasting where there is a point-to-multipoint transmission can be used in interactive services. Users connected in a narrowband mobile-communications network can enter into the appropriate high-speed area and download the requested data. Two important issues of hybrid systems are the service availability and the scalability [8]. Several projects have recently been realized in Europe. Among these are MEMO (DAB/GSM), SABINA (DVB-T/GSM) and MCP (Multimedia Car Platform) [9-11], specifying network architectures that combine broadcast and mobile-communication systems.

In this paper, a broadband wireless asymmetric system is presented. The system makes use of GPS/GSM/DVB-T [Global Positioning System/Global System for Mobile Communications/ Digital Video Broadcasting-Terrestrial] technologies. A base station, called a high-speed station (HSS), transmits information in the form of DVB [12]. The transmission direction depends on the user's position. All mobile units are equipped with GPS receivers to provide accurate, continuous, worldwide, three-dimensional position and velocity information [13]. The information is translated and subsequently transmitted to the high-speed station through GSM (uplink), in the form of an SMS [short messaging service] message. The message also contains the request for the data to be transmitted from the high-speed station. After the appropriate processing, the high-speed station transmits the data in the form of DVB to the user. The transmitter of the high-speed station can work in the ISM band, or in any other appropriate frequency band. The high-speed station contains a "smart antenna," which directs the beams to the users' positions. In the application layer, TCP/IP is used.

The data link is realized according to RFC 3077 [14], while the packed encapsulation follows RFC 2784. The physical layer is compatible with DVB-T, where EN 301192 [12] is used. The network management follows international standards; DVB-T should be seen as a complementary technology not only to GSM but also to UMTS [15]. The service availability of DVB-T could make the Mobile Internet Package friendly to users. A simple diagram of the envisaged network is shown in Figure 1.

The mobile-unit equipment (Figure 2) includes a GPS receiver, a GSM terminal, a DVB receiver, a notebook, and three antennas (GPS, GSM, DVB). The high-speed station equipment comprises a computer, a GSM terminal, the digital logic and the memory unit, the switch drivers, the beamforming network, a DVB-T transmitter, a GPS receiver (optional), two omnidirectional antennas, and a smart antenna. Figure 3 presents the block diagram of the high-speed station.

3. The Switched-Beam Smart Antenna

It is well known that electronically steerable directive antennas have no moving parts. Due to this, fast beam switching is possible, which allows multibeam plus multi-frequency support of the communications system. As the antenna beam becomes narrower, the carrier-to-interference ratio (C/I) increases. Currently, there are more than 1.2 million commercial cell sites worldwide. It is expected that this number will increase five times in the next five years. Among them, the broadband sites with corresponding antennas will share important growth.

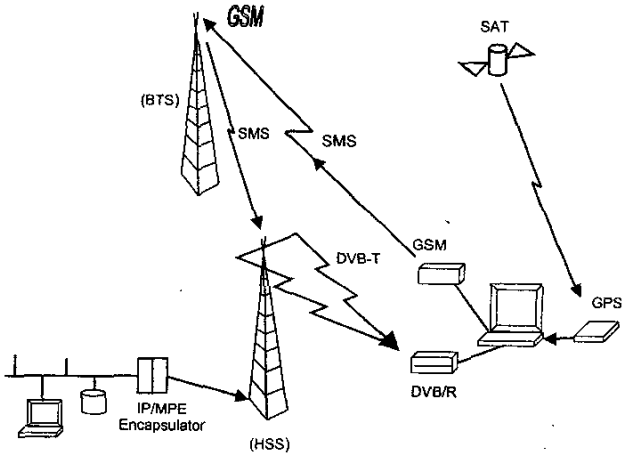

Figure 1. An asymmetric broadband wireless network.

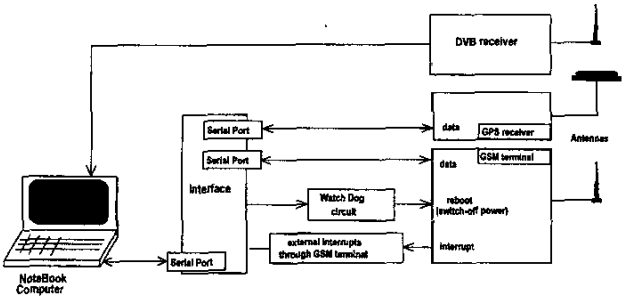

Figure 2. The mobile-unit equipment.

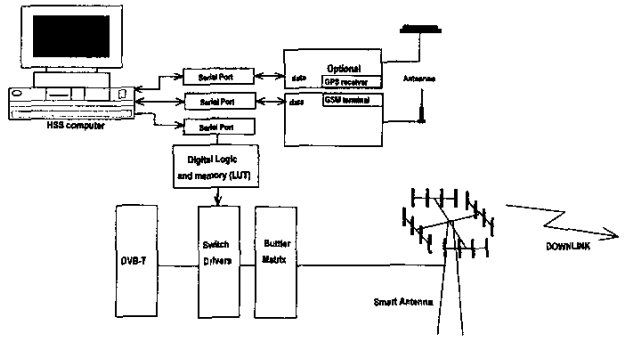

Figure 3. The high-speed station (HSS) equipment.

Our work combines a switched-beam broadband antenna with a beamformer introduced at the RF stage. A circuit topology that provides the specific phase sequences to the antenna elements is proposed. This task can be realized by a Butler [16] or a Blass [17] matrix. A combination of 90° hybrids and suitable phase shifters creates the Butler matrix (BM) beamforming network. The Butler matrix provides an equal number, $N = 2^n$, of inputs and outputs. N is also the number of the orthogonally linear independent beams coming from the spatial Fourier transform.

An 8 × 8 Butler matrix is presented in Figure 4. The rectangles of the first and the last column represent the input and the output ports, respectively. The X-shaped components correspond to ideal 3 dB hybrids, in which the secondary output either leads or lags the primary output by 90°. The inner rectangles represent the phase shifters. Inputs are marked as "iR" or "iL," where $i = 1,2,3,4$. R and L stand for right and left, respectively. Thus, the $2R$ input produces excitations that generate the second uniform beam to the right. For the 8 × 8 Butler matrix we have eight possible orthogonal beams, shown in Figure 5a. The angular coverage is about 120°, and the sidelobe level is less than −11.5 dB. For a desired sidelobe level less than −20 dB, a combination of two equal inputs can be implemented. The input/output excitations for the 8 × 8 Butler matrix are presented in Table 1. Figure 5b shows the radiation patterns of seven different excitations. It is noted that grating lobes appear in the 0° and 180° directions. This is true only for arrays with point sources. For most arrays with actual elements, the above lobes disappear. In practice, the elements of the antenna could be microstrip patches or dipoles in front of a planar reflector.

When using the above excitations, the number of simultaneous beams from a given array is typically limited. One could combine the amplitude at the input ports to increase the number of beams. So instead of applying the same excitation to the consecutive inputs, different excitations can be used. A switch-matrix-feeding example is presented in Figure 6. $2L$, $1L$, $1R$, and $2R$ are the output ports, which are connected to the respective inputs of the 4 × 4 Butler matrix. S_1, S_2, S_3, S_4, S_5, S_6, S_7, S_8, S_9, and S_{10} are SPDT switches that combine the inputs. All switches are shown in logic state "1". S_1 and S_2 are switches for path selection. Path S_1, S_2, A_3 is a direct path from the input to any single output. A second path, S_1, S_2, A_2, B_2, equally divides the input power among any pair of outputs. Finally, a third path,

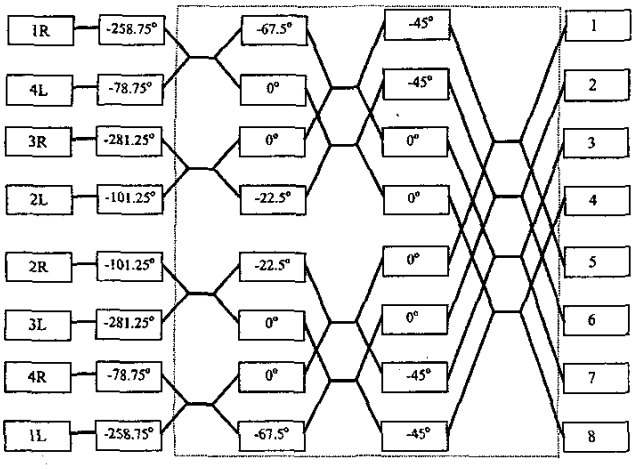

Figure 4. An 8 × 8 Butler matrix.

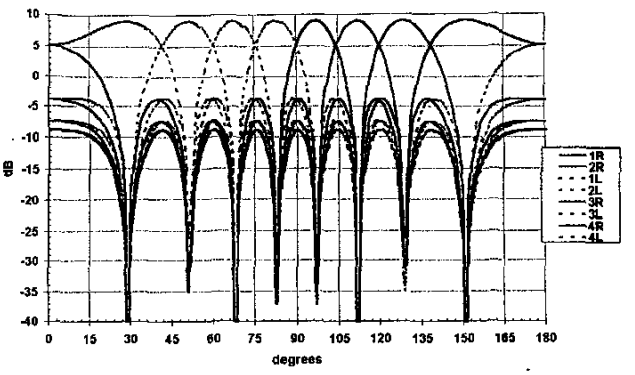

Figure 5a. Eight independent beams with uniform illumination, obtained from a linear array of eight radiating elements fed by an 8 × 8 Butler matrix. The element spacing is $\lambda/2$.

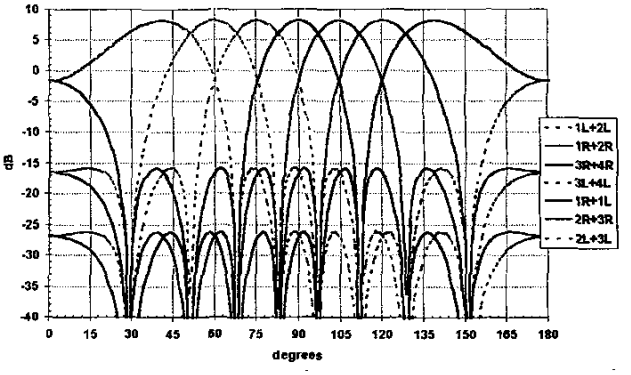

Figure 5b. The formation of seven cosine illumination by the addition of uniform beams.

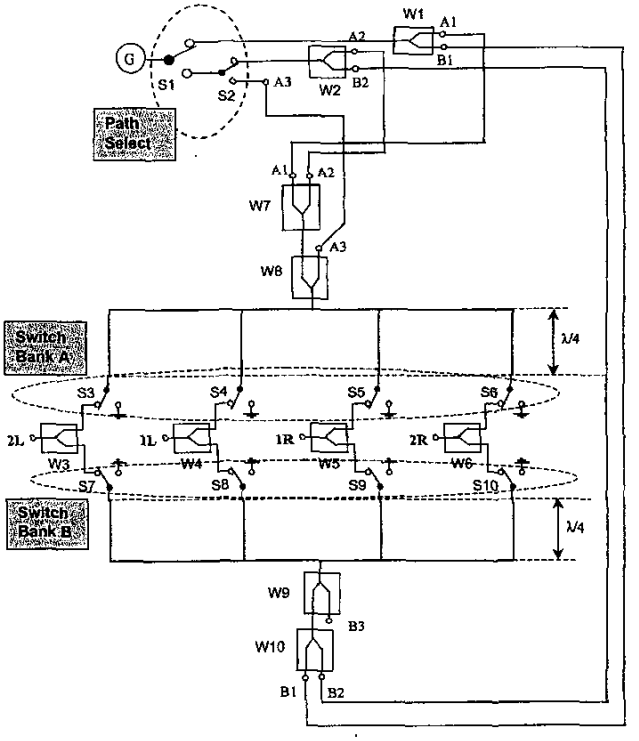

Figure 6. The switch matrix feeding the 4 × 4 Butler matrix.

Table 1a. The input amplitudes and resulting output excitations from an 8 × 8 Butler-matrix feed network for uniform-illumination beams.

		1R (+22.5°)		4L (–157.5°)		3R (+112.5°)		2L (–67.5°)	
		Mag	Phase	Mag	Phase	Mag	Phase	Mag	Phase
Input Port	1	1	0	0	0	0	0	0	0
	2	0	0	1	0	0	0	0	0
	3	0	0	0	0	1	0	0	0
	4	0	0	0	0	0	0	1	0
	5-8	0	0	0	0	0	0	0	0
Output Port	1	0.35355	78.75	0.35355	168.75	0.35355	33.75	0.35355	123.75
	2	0.35355	56.25	0.35355	–33.75	0.35355	–78.75	0.35355	–168.75
	3	0.35355	33.75	0.35355	123.75	0.35355	168.75	0.35355	–101.25
	4	0.35355	11.25	0.35355	–78.75	0.35355	56.25	0.35355	–33.75
	5	0.35355	–11.25	0.35355	78.75	0.35355	–56.25	0.35355	33.75
	6	0.35355	–33.75	0.35355	–123.75	0.35355	–168.75	0.35355	101.25
	7	0.35355	–56.25	0.35355	33.75	0.35355	78.75	0.35355	168.75
	8	0.35355	–78.75	0.35355	–168.75	0.35355	–33.75	0.35355	–123.75

		2R (+67.5°)		3L (–112.5°)		4R (+157.5°)		1L (-22.5°)	
		Mag	Phase	Mag	Phase	Mag	Phase	Mag	Phase
Input Port	1-4	0	0	0	0	0	0	0	0
	5	1	0	0	0	0	0	0	0
	6	0	0	1	0	0	0	0	0
	7	0	0	0	0	1	0	0	0
	8	0	0	0	0	0	0	1	0
Output Port	1	0.35355	–123.75	0.35355	–33.75	0.35355	–168.75	0.35355	–78.75
	2	0.35355	168.75	0.35355	78.75	0.35355	33.75	0.35355	–56.25
	3	0.35355	101.25	0.35355	–168.75	0.35355	–123.75	0.35355	–33.75
	4	0.35355	33.75	0.35355	–56.25	0.35355	78.75	0.35355	–11.25
	5	0.35355	–33.75	0.35355	56.25	0.35355	–78.75	0.35355	11.25
	6	0.35355	–101.25	0.35355	168.75	0.35355	123.75	0.35355	33.75
	7	0.35355	–168.75	0.35355	–78.75	0.35355	–33.75	0.35355	56.25
	8	0.35355	123.75	0.35355	33.75	0.35355	168.75	0.35355	78.75

Table 1b. The input amplitudes and resulting output excitations from an 8 × 8 Butler matrix that generates a set of four simultaneous cosine-shaped illuminations. The phase increments of the output-port excitations are ±45° and ±135°.

		1R+2R (+45°)		3R+4R (+135°)		1L+2L (–45°)		3L+4L (–135°)	
		Mag	Phase	Mag	Phase	Mag	Phase	Mag	Phase
Input Port	1	0.707107	0	0	0	0	0	0	0
	2	0	0	0	0	0	0	0.707107	0
	3	0	0	0.707107	0	0	0	0	0
	4	0	0	0	0	0.707107	0	0	0
	5	0.707107	0	0	0	0	0	0	0
	6	0	0	0	0	0	0	0.707107	0
	7	0	0	0.707107	0	0	0	0	0
	8	0	0	0	0	0.707107	0	0	0
Output Port	1	0.09755	157.5	0.09755	112.5	0.09755	–157.5	0.09755	–112.5
	2	0.27779	112.5	0.27779	–22.5	0.27779	–112.5	0.27779	22.5
	3	0.41573	67.5	0.41573	–157.5	0.41573	–67.5	0.41573	157.5
	4	0.49039	22.5	0.49039	67.5	0.49039	–22.5	0.49039	–67.5
	5	0.49039	–22.5	0.49039	–67.5	0.49039	22.5	0.49039	67.5
	6	0.41573	–67.5	0.41573	157.5	0.41573	67.5	0.41573	–157.5
	7	0.27779	–112.5	0.27779	22.5	0.27779	112.5	0.27779	–22.5
	8	0.09755	–157.5	0.09755	–112.5	0.09755	157.5	0.09755	112.5

Table 1c. The input amplitudes and resulting output excitations from an 8 × 8 Butler matrix that generates a second set of three simultaneous cosine-shaped illuminations. The phase increments of the output-port excitations are 0° and ±90°.

		2R+3R (+90°)		2L+3L (–90°)		1R+1L (0°)	
		Mag	Phase	Mag	Phase	Mag	Phase
Input Port	1	0	0	0	0	0.707106781	0
	2	0	0	0	0	0	0
	3	0.707106781	0	0	0	0	0
	4	0	0	0.707106781	0	0	0
	5	0.707106781	0	0	0	0	0
	6	0	0	0.707106781	0	0	0
	7	0	0	0	0	0	0
	8	0	0	0	0	0.707106781	0
Output Port	1	0.09755	–45	0.09755	45	0.09755	0
	2	0.27779	–135	0.27779	135	0.27779	0
	3	0.41573	135	0.41573	–135	0.41573	0
	4	0.49039	45	0.49039	–45	0.49039	0
	5	0.49039	–45	0.49039	45	0.49039	0
	6	0.41573	–135	0.41573	135	0.41573	0
	7	0.27779	135	0.27779	–135	0.27779	0
	8	0.09755	45	0.09755	–45	0.09755	0

Table 2. A list of the 10-bit control-word settings and the corresponding 4 × 4 Butler-matrix (BM) excitations resulting in the beam patterns shown in Figure 7. The rows in gray are optional settings used only in switch-matrix symmetry measurements.

	Path Select Switches		Switch Bank A				Switch Bank B				4 × 4 BM Active Ports	Beam
	S1	S2	S3	S4	S5	S6	S7	S8	S9	S10		
1:0 path	0	0	0	0	1	0	0	0	0	0	1R	R3 1:0
	0	0	0	0	0	1	0	0	0	0	2R	R4 1:0
	0	0	0	1	0	0	0	0	0	0	1L	L1 1:0
	0	0	1	0	0	0	0	0	0	0	2L	L2 1:0
1:1 path	0	1	0	1	0	0	0	0	1	0	1R + 1L	L13 1:1
	0	1	0	0	1	0	0	1	0	0		
	0	1	0	0	1	0	0	0	0	1	1R + 2R	R34 1:1
	0	1	0	0	0	1	0	0	1	0		
	0	1	0	1	0	0	1	0	0	0	1L + 2L	L12 1:1
	0	1	1	0	0	0	0	1	0	0		
1:2 and 2:1 paths	1	X	0	0	1	0	0	1	0	0	1R (0 dB) + 1L (–3 dB)	R13 1:2
	1	X	0	0	0	1	0	0	1	0	2R (0 dB) + 1R (-3 dB)	R34 1:2
	1	X	0	0	1	0	0	0	0	1	1R (0 dB) + 2R (-3 dB)	R34 2:1
	1	X	0	1	0	0	1	0	0	0	1L (0 dB) + 2L (-3 dB)	L12 2:1
	1	X	1	0	0	0	0	1	0	0	2L (0 dB) + 1L (-3 dB)	L12 1:2
	1	X	0	1	0	0	0	0	1	0	1L (0 dB) + 1R (-3 dB)	L13 2:1

S_1, S_2, A_i, B_1, unequally divides the input power among any pair of outputs. S_3, S_4, S_5, S_6, S_7, S_8, S_9, and S_{10} select the desired outputs and isolate the unused ports. W_i, $i = 1,...,10$ represent Wilkinson-type dividers or combiners. W_1 performs unequal power division between outputs ($P_{A1} = 2P_{B1}$). W_2, W_7, W_8, W_9, and W_{10} are typical 3 dB dividers, while W_3, W_4, W_5, and W_6 are utilized as power combiners. A 10-bit digital word defines which port combination is active, and specifies the corresponding excitation levels of selected outputs. The switching combinations are given in Table 2. Any single port or pair of ports can be selected. The port excitations can be either low (–3 dB) or high (0 dB) level. The 10-bit word is transferred from a processor that decodes the information about the user's position. If, for example, it is desired to have the relative excitations $1R = 0$ dB, $1L = -3$ dB while $2L$ and $2R$ are open, the digital word will be

$$S_1, S_2, S_3, S_4, S_5, S_6, S_7, S_8, S_9, S_{10} \rightarrow 1X00100100,$$

where X denotes that the bit is not used.

Figure 7 presents the possible patterns obtained by the non-uniform addition of the uniform beams of a 4 × 4 Butler matrix. The working linear array consists of four parallel dipoles. The inter-element distance is $\lambda/2$, and the array is positioned $\lambda/4$ away from a planar reflector. The ratio of the excitations among the consecutive inputs is

1:0, 2:1, 1:1, and 1:2.

1:0 corresponds to single-port excitation of the Butler-matrix network, while 1:1 corresponds to a dual-port excitation with equal amplitudes. 2:1 and 1:2 are also dual-port excitations, but with a 3 dB difference in amplitude levels. Table 2 explains the notation used in the diagrams of Figure 7.

In total, the array can produce 13 beams within a 120° sector. An equilateral-trihedral prism, containing the above array in each face, constitutes an antenna that is able to scan three 120° sectors. The switches presented in Figure 6 and the whole design can be based on Mini-Circuits RSW-2-25P or TOSW-230 switches [20] or similar components. Details on circuit connections for two switches (S_5, S_6) are shown in Figure 8.

An 8 × 8 Butler matrix with the same excitations as above can also cover a 120° sector. Again, an equilateral-trihedral prism containing an eight-parallel-dipole linear array in each face constitutes an antenna able to scan 360° of sectors. Figure 9 presents a diagram of the array, and Figure 10 shows the corresponding patterns in one face. Table 3 explains the notation in the diagrams of Figure 10.

It is helpful to give a visual presentation of the performance of the above two arrays. Figure 11 shows the direction of the main lobe versus sidelobe level and half-power beamwidth for a 4 × 4 and an 8 × 8 parallel-dipole array. A variation of the sidelobe level for both arrays is observed from this figure. By applying constraints on the sidelobe level and taking into account the half-power beamwidth, it can be concluded that the number of different excitations and beams can be reduced. If a sidelobe level of less

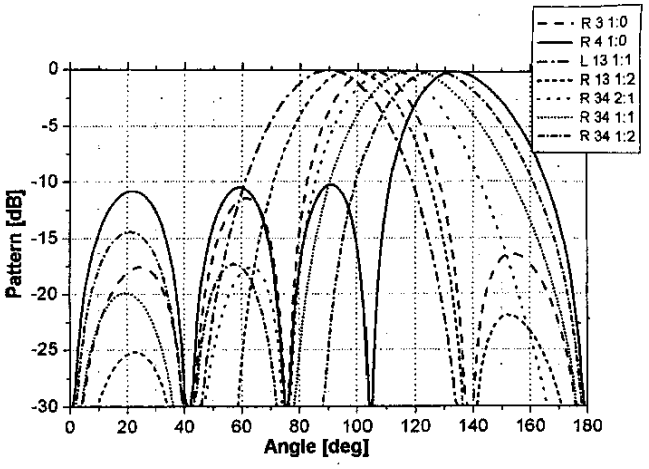

Figure 7a. The beam patterns obtained by non-uniform addition of uniform beams in a 4 × 4 Butler matrix, using the right inputs.

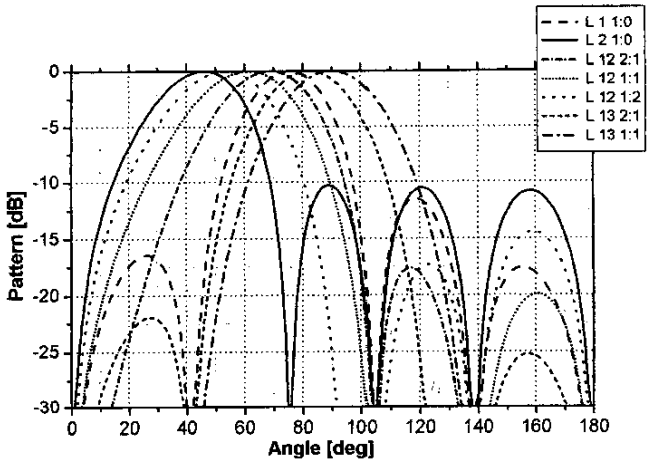

Figure 7b. The beam patterns obtained by non-uniform addition of uniform beams in a 4 × 4 Butler matrix, using the left inputs.

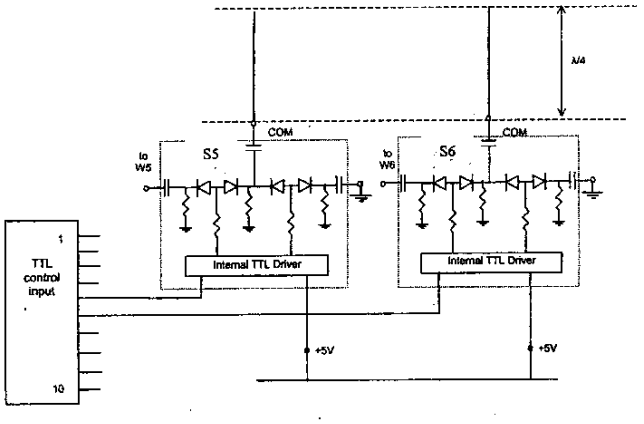

Figure 8. The details of the Butler-matrix feed design.

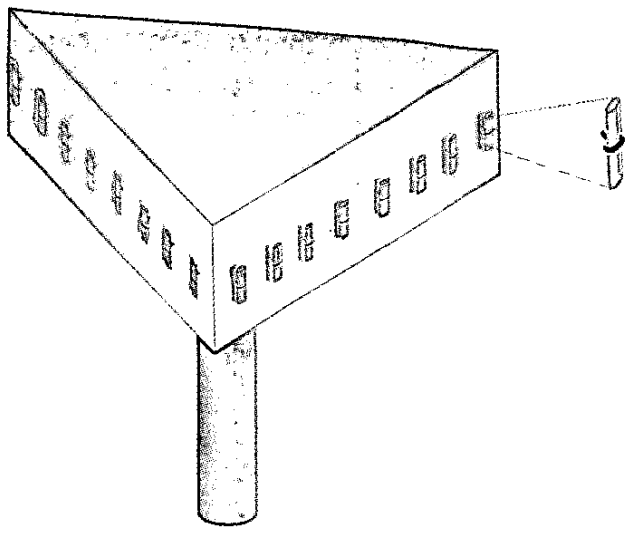

Figure 9. A diagram of a three-face twenty-four dipole array.

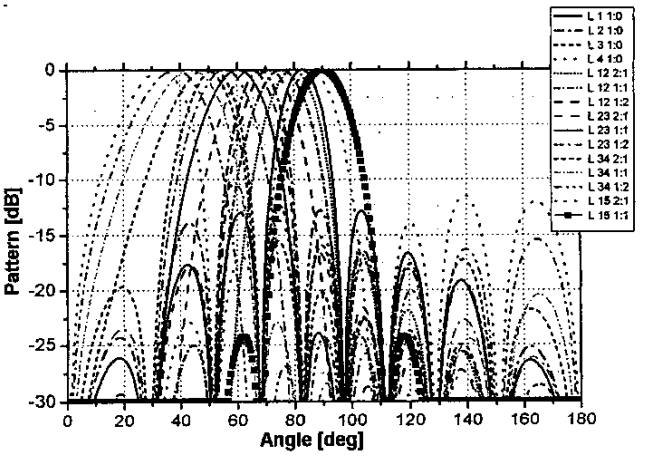

Figure 10a. The beam patterns obtained by non-uniform addition of uniform beams in an 8 × 8 Butler matrix, using the L inputs.

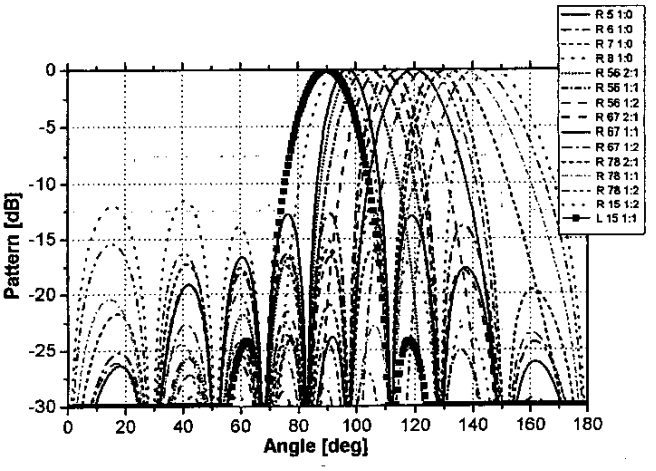

Figure 10b. The beam patterns obtained by non-uniform addition of uniform beams in an 8 × 8 Butler matrix, using the R inputs.

Table 3. A list of the 18-bit control-word settings and the corresponding 8 × 8 Butler-matrix (BM) excitations resulting in the beam patterns shown in Figure 10.

	Path Select Switches		Switch Bank A								Switch Bank B								8 × 8 BM Active Ports	Beam
	S1	S2	S3	S4	S5	S6	S7	S8	S9	S10	S11	S12	S13	S14	S15	S16	S17	S18		
1:0 Path	0	0	1	0	0	0	0	0	0	0	0	0	0	0	0	0	0	0	4L	L4 1:0
	0	0	0	1	0	0	0	0	0	0	0	0	0	0	0	0	0	0	3L	L3 1:0
	0	0	0	0	1	0	0	0	0	0	0	0	0	0	0	0	0	0	2L	L2 1:0
	0	0	0	0	0	1	0	0	0	0	0	0	0	0	0	0	0	0	1L	L1 1:0
	0	0	0	0	0	0	1	0	0	0	0	0	0	0	0	0	0	0	1R	R5 1:0
	0	0	0	0	0	0	0	1	0	0	0	0	0	0	0	0	0	0	2R	R6 1:0
	0	0	0	0	0	0	0	0	1	0	0	0	0	0	0	0	0	0	3R	R7 1:0
	0	0	0	0	0	0	0	0	0	1	0	0	0	0	0	0	0	0	4R	R8 1:0
1:1 Path	0	1	0	0	0	0	1	0	0	0	0	0	0	1	0	0	0	0	1R + 1L	L15 1:1
	0	1	0	0	0	0	1	0	0	0	0	0	0	0	0	1	0	0	1R + 2R	R56 1:1
	0	1	0	0	0	0	0	1	0	0	0	0	0	0	0	0	1	0	2R + 3R	R67 1:1
	0	1	0	0	0	0	0	0	1	0	0	0	0	0	0	0	0	1	3R + 4R	R78 1:1
	0	1	0	0	0	1	0	0	0	0	0	0	1	0	0	0	0	0	1L + 2L	L12 1:1
	0	1	0	0	1	0	0	0	0	0	0	1	0	0	0	0	0	0	2L + 3L	L23 1:1
	0	1	0	1	0	0	0	0	0	0	1	0	0	0	0	0	0	0	3L + 4L	L34 1:1
1:2 and 2:1 Paths	1	X	0	0	0	1	0	0	0	0	0	0	1	0	0	0	0	0	1L(0 dB) + 2L(–3 dB)	L12 2:1
	1	X	0	0	1	0	0	0	0	0	0	0	0	1	0	0	0	0	2L(0 dB) + 1L(–3 dB)	L12 1:2
	1	X	0	0	1	0	0	0	0	0	0	1	0	0	0	0	0	0	2L(0 dB) + 3L(–3 dB)	L23 2:1
	1	X	0	1	0	0	0	0	0	0	0	0	1	0	0	0	0	0	3L(0 dB) + 2L(–3 dB)	L23 1:2
	1	X	0	1	0	0	0	0	0	0	1	0	0	0	0	0	0	0	3L(0 dB) + 4L(–3 dB)	L34 2:1
	1	X	1	0	0	0	0	0	0	0	0	1	0	0	0	0	0	0	4L(0 dB) + 3L(–3 dB)	L34 1:2
	1	X	0	0	0	1	0	0	0	0	0	0	0	0	1	0	0	0	1L(0 dB) + 1R(–3 dB)	L15 2:1
	1	X	0	0	0	0	1	0	0	0	0	0	0	0	0	1	0	0	1R(0 dB) + 2R(–3 dB)	R56 2:1
	1	X	0	0	0	0	0	1	0	0	0	0	0	0	1	0	0	0	2R(0 dB) + 1R(–3 dB)	R56 1:2
	1	X	0	0	0	0	0	1	0	0	0	0	0	0	0	0	1	0	2R(0 dB) + 3R(–3 dB)	R67 2:1
	1	X	0	0	0	0	0	0	1	0	0	0	0	0	0	1	0	0	3R(0 dB) + 2R(–3 dB)	R67 1:2
	1	X	0	0	0	0	0	0	1	0	0	0	0	0	0	0	0	1	3R(0 dB) + 4R(–3 dB)	R78 2:1
	1	X	0	0	0	0	0	0	0	1	0	0	0	0	0	0	1	0	4R(0 dB) + 3R(–3 dB)	R78 1:2
	1	X	0	0	0	0	1	0	0	0	0	0	0	1	0	0	0	0	1R(0 dB) + 1L(–3 dB)	R15 1:2

than −19 dB is desired for a 4 × 4 array, only the 1:1 excitation can be used. In this case, three beams that cover a 90° sector are generated. A square tetrahedron containing four dipoles in each face is able to scan the whole space. It is noticed that in any case, the half-power beamwidth and the sidelobe level (Figure 11) define the possible number of excitations and the beams.

4. Narrow-Beam Antenna Performance

It is well known that in a real environment the effective antenna gain is not exactly the same as the free-space value in the corresponding direction, due to multipath propagation. The effective antenna gain can be defined [18] as the quotient of the power received in the narrow beam, P_n, and the power received by a collocated omnidirectional antenna, P_0. The two powers are averaged over the fast fading (E_{FF}), and thus

$$e = \frac{E_{FF}\{P_n\}}{E_{FF}\{P_0\}}. \qquad (1)$$

The effective antenna gain and the difference between the physical angle and the angle of arrival from the high-speed station to the user show that there is a strong correlation among the above quantities. The main lobe in a real environment and the dominant angles of arrival (DOA) are slightly different compared to the free-space case. Obviously, one can assume that the sighting angles obtained with the help of the GPS data correspond to real values. The angle of arrival (*AoA*) from the high-speed station to the mobile unit in the line-of-sight (*LoS*) case typically follows the beam of the antenna pattern. For the non-line-of-sight (*NLoS*) case, there is no direct path. However, measurements and model predictions [19] show that a significant power percentage still remains in the main lobe of the antenna. At the same time, an angular spread appears in the high-speed-station antenna beam.

The performance of the forward channel is considered significant, mainly because of its rich content. If the reverse and the forward channels operate at the same frequency, an adaptive array for the is considered significant could be a suitable choice. That happens because adaptive beamforming avoids the multipath-fading problem. For asymmetric wireless networks, the reverse channel operates at a frequency different from the forward channel and with much less bandwidth. Since the adaptive systems are

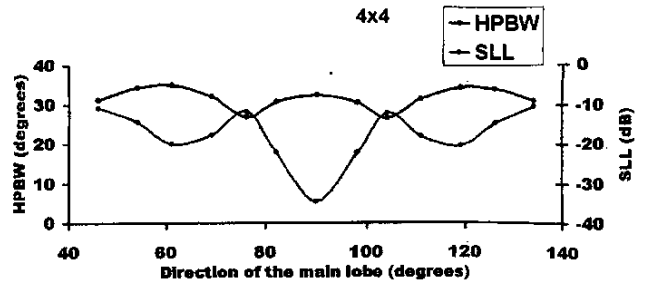

Figure 11a. The half-power beamwidths and sidelobe levels of the beams obtained by the non-uniform addition of uniform beams in a 4 × 4 Butler matrix.

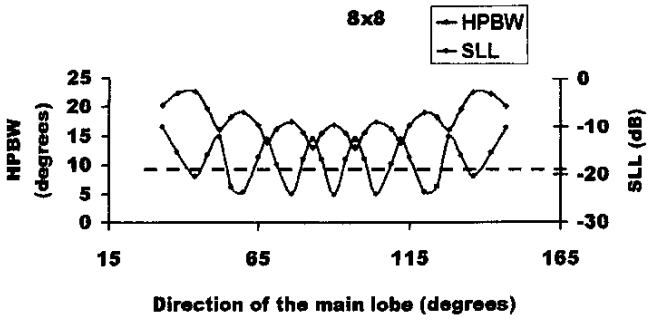

Figure 11b. The half-power beamwidths and sidelobe levels of the beams obtained by the non-uniform addition of uniform beams in a 8 × 8 Butler matrix.

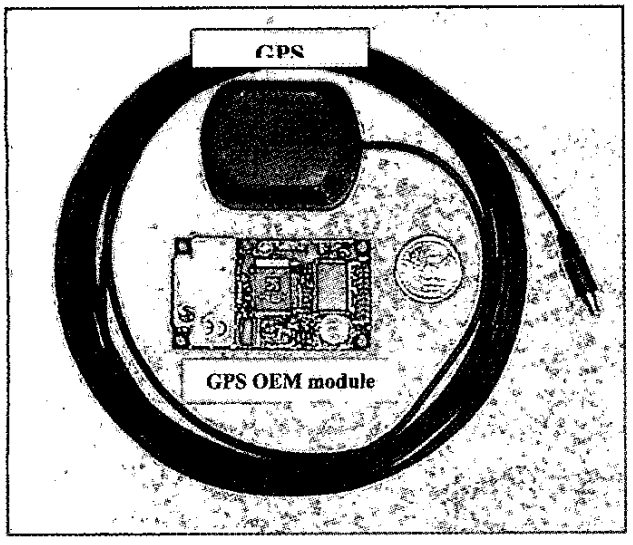

Figure 12. The GPS module.

based on measurements of the reverse channel, such measurements in asymmetric wireless networks do not accurately fit the forward channel. There is thus an uncertainty in the system's performance, which increases with the frequency difference of the two channels. In this case, it seems that a switched-beam array with a GPS system offers an alternative and attractive solution.

One issue that arises has to do with the interference with other mobile units produced by the signal of the high-speed station. Let us assume that a 4 × 4 Butler matrix with nonuniform excitation is used. The targeted mobile user is at 60°, while another user is at 161°. It is desired that the second user receive the minimum possible radiation. To solve this problem, one way is to apply the 1:1 excitation of $1R$ plus $2R$. In this case, the interference level with respect to the maximum of radiation is −20 dB. Another solution that can be suggested uses the 2:1 excitation, for which we have a relative radiation level of −0.83 dB toward the desired direction, whereas the level becomes −47.8 dB toward the undesired direction. The second case is obviously much better than the first case. It is noted that in practice we do have a lot of undesired users, and the choice of the excitation will be realized by taking into account their positions. Co-channel interference is one of the main reasons for link degradation. In our case, power control in conjunction with the beam switch can improve the link performance. The power control is adjusted by using the GPS information.

5. User Monitoring

The concept of user monitoring is based on the Global Positioning System (GPS). Each user is equipped with a GPS receiver, which runs under an appropriate controller and calculates its current position. The data required by the receiver are the longitude and the latitude at a specific time. Based on the GSM infrastructure, a return path from the user back to the high-speed station will be required. The position of the user is transmitted in digital form by using the sort message service (SMS) of the GSM system. Each user transmits an SMS, which is stored at the high-speed station.

The equipment is powered by an appropriate supply unit at the mobile unit (user). The equipment is powered by its generator if the user is on a vehicle. The generator charges a 12 volt battery, which prevents the voltage from dropping or disconnecting. The GPS receiver can be any type available in the market, with a power consumption of 1.2 mW at the most.

The high-speed-station software uses a client/server architecture. It handles one database with the past itineraries and another with the users. In addition, the server keeps information about client connections. The server collects data from the users via the GSM terminal. The access is achieved through a client-station after authentication control.

The monitoring is based on a fleet system that has recently been given [21]. Figure 12 presents the GPS module (receiver and GSM terminal) as it was synthesized to be used in the network.

6. Summary

In this paper, a switched-beam wideband base station has been presented. The station can provide services to both mobile and residential subscribers. Additionally, small- and medium-sized enterprises (SME), as well as small offices/home offices (SOHO), can be served. The main services can be high-speed Internet access, video-streaming services, and IP telephony. Our topology makes use of two schemes. One has four sectors, each with 90° angular coverage, and the other has three sectors of 120° each. The base-station antenna can produce more switched beams than the classical Butler matrix. The number of simultaneous beams increases by combining the relative amplitudes of the input ports. The circuits, as well as the schematic diagram of the feed network, have been analyzed and presented. The direction of the user and

his/her distance from base station are found via GPS. Our system can be considered to be a hybrid, since it combines benefits and tradeoffs of both switched-beam and adaptive arrays.

7. References

1. G. V. Tsoulos (ed.), *Adaptive Antennas for Wireless Communications*, Piscataway, IEEE Press, 2001.

2. T. S. Rappaport (ed.), *Smart Antennas*, New York, IEEE Press, 1998.

3. R. C. Hansen, *Phased Array Antennas*, New York, Wiley-Interscience, 1998.

4. R. T. Compton, Jr., *Adaptive Antennas*, Englewood Cliffs, New Jersey, Prentice-Hall, 1988.

5. C. .B. Dietrich, Jr. and W. L. Stutzman, "Smart Antennas Enhance Cellular/PCS Performance, Parts I and II," *Microwaves and RF*, April and May, 1997, pp. 76-86 and pp. 164-168.

6. M. Chryssomallis, "Smart Antennas," *IEEE Antennas and Propagation Magazine*, **42**, 3, 2000, pp. 129-136.

7. C. B. Dietrich, Jr., W. L. Stutzman, B. Kim, and K. Dietze, "Smart Antennas in Wireless Communications: Base-Station Diversity and Handset Beamforming," *IEEE Antennas and Propagation Magazine*, **42**, 5, 2000, pp. 142-151.

8. O. Moniya, M. Serizawa, and K. Kobayashi, "Service Performance Analysis of Spot-Area Hybrid Multimedia Mobile Communication System," Proceedings of the 51st IEEE Vehicular Technology Conference 2000, Session 6.11-2.

9. J. Ossfeldt, "RVK99: MEMO Brings DAB into Interactive Mobile Multimedia," Teracom AB, Sweden, 1998.

10. M. Andersson, "MEMO/DVB-T Prototype," ACTS 0054, European Union, 1999.

11. E. Stare and S. Lindren, "Hybrid Broadcast – Telecom Systems for Spectrum Efficient Mobile Broadband Internet Access," Teracom AB, Sweden, 2000.

12. "Digital Video Broadcasting (DVB); DVB Specification for Data Broadcasting," ETSI EN 301192 (1997-12) European Standard (Telecommunications Series).

13. E. D. Kaplan, Understanding GPS Principles and Applications, Norwood, MA, Artech House Inc., 1996.

14. RFC 3077.

15. F. Muratore, "UMTS Mobile Communications for the Future," New York, John Wiley & Sons Ltd., 2001.

16. J. L. Butler, "Digital Matrix and Intermediate Frequency Scanning" in R. C. Hansen (ed.), *Microwave Scanning Antennas*, Peninsula Publishing, 1985, Chapter 3.

17. J. Blass, "Multidirectional Antenna: A New Approach to Stacked Beams," IRE International Conference Record, 8 (Part 1), 1960.

18. P. Zetterberg, "Performance of Narrow-Beams in a Suburban Environment," Proceedings of the 51st IEEE Vehicular Technology Conference 2000, Session 1.07-5.

19. L. M. Correia, *Wireless Flexible Personalized Communications*, New York, John Willey & Sons, 2001.

20. http://www.miniciruits.com

21. C. S. Koukourlis, S. S. Spyridakis, and N. V. Kokkalis, "On the Design of a Fleet Monitoring System with Reduced Power Consumption," *Elect. Eng.*, **84**, 2002, pp. 203-210.